Mechanism by Which Fatty Acids Inhibit Insulin Activation of Insulin Receptor Substrate-1 (IRS-1)-associated Phosphatidylinositol 3-Kinase Activity in Muscle*

Chunli Yu‡§, Yan Chen‡§¶, Gary W. Cline‡, Dongyan Zhang‡¶, Haihong Zong‡, Yanlin Wang‡¶, Raynald Bergeron‡, Jason K. Kim¶, Samuel W. Cushman‖, Gregory J. Cooney, Bronwyn Atcheson**, Morris F. White‡‡§§, Edward W. Kraegen**, and Gerald I. Shulman‡¶§§¶¶‖‖**

*From the ‡Departments of Internal Medicine and ¶¶Cellular and Molecular Physiology and the ¶Howard Hughes Medical Institute, Yale University School of Medicine, New Haven, Connecticut 06510, ‖NIDDK, National Institutes of Health, Bethesda, Maryland 20814, ‡‡Howard Hughes Medical Institute, Joslin Diabetes Center, Harvard Medical School, Boston, Massachusetts 02215, and **Garvan Institute of Medical Research, Sydney, New South Wales, Australia*

Recent studies have demonstrated that fatty acids induce insulin resistance in skeletal muscle by blocking insulin activation of insulin receptor substrate-1 (IRS-1)-associated phosphatidylinositol 3-kinase (PI3-kinase). To examine the mechanism by which fatty acids mediate this effect, rats were infused with either a lipid emulsion (consisting mostly of 18:2 fatty acids) or glycerol. Intracellular C18:2 CoA increased in a time-dependent fashion, reaching an ~6-fold elevation by 5 h, whereas there was no change in the concentration of any other fatty acyl-CoAs. Diacylglycerol (DAG) also increased transiently after 3–4 h of lipid infusion. In contrast there was no increase in intracellular ceramide or triglyceride concentrations during the lipid infusion. Increases in intracellular C18:2 CoA and DAG concentration were associated with protein kinase C (PKC)-θ activation and a reduction in both insulin-stimulated IRS-1 tyrosine phosphorylation and IRS-1 associated PI3-kinase activity, which were associated with an increase in IRS-1 Ser[307] phosphorylation. These data support the hypothesis that an increase in plasma fatty acid concentration results in an increase in intracellular fatty acyl-CoA and DAG concentrations, which results in activation of PKC-θ leading to increased IRS-1 Ser[307] phosphorylation. This in turn leads to decreased IRS-1 tyrosine phosphorylation and decreased activation of IRS-1-associated PI3-kinase activity resulting in decreased insulin-stimulated glucose transport activity.

Insulin resistance in skeletal muscle is a major factor in the pathogenesis of type 2 diabetes. Recent studies in animals and humans have demonstrated a strong relationship with increased intramuscular triglyceride content (1–4) and intramyocellular triglyceride content as assessed by ^{1}H NMR

(5–7). In addition, infusions of lipid emulsions with heparin to acutely raise plasma fatty acid concentrations have also been shown to cause profound insulin resistance in rat and human skeletal muscle within 4–6 h (8–11). The mechanism by which fatty acids induce insulin resistance in skeletal muscle remains controversial. Randle *et al.* (12, 13) first suggested that fatty acids might induce insulin resistance in skeletal muscle by inhibiting pyruvate dehydrogenase activity, resulting in an increase in intracellular citrate concentration, which would then result in inhibition of phosphofructokinase activity leading to an increase in intracellular glucose-6-phosphate; this in turn would inhibit hexokinase activity, resulting in decreased glucose uptake. More recent ^{31}P/^{13}C NMR studies in humans have revealed a very different mechanism of fatty acid-induced insulin resistance whereby an increase in plasma fatty acid concentration was shown to result in lower intramyocellullar glucose 6-phosphate (9, 14) and glucose concentrations (10), suggesting that fatty acids inhibit insulin-stimulated glucose transport activity (10). These changes were associated with reduced insulin-stimulated IRS-1[1] tyrosine phosphorylation (11) and IRS-1-associated phosphatidylinositol 3-kinase (PI3-kinase) activity (10, 11) suggesting that fatty acids cause insulin resistance through inhibition of insulin signaling, which we hypothesized might occur through activation of a serine kinase cascade involving PKC-θ (11). To explore the possible roles of different intracellular fatty acid metabolites such as fatty acyl-CoA, diacylglycerol (DAG), ceramides, and triglycerides in mediating fatty acid-induced insulin resistance in skeletal muscle, we measured these metabolites at different time intervals during a lipid infusion in relation to insulin stimulation: (i) insulin receptor tyrosine phosphorylation, (ii) IRS-1 tyrosine phosphorylation, and (iii) IRS-1-associated PI3-kinase activity as well as PKC-θ translocation. In a separate group of *in vitro* soleus muscle studies, we also examined whether fatty acid-induced defects in insulin signaling were coupled to defects in insulin-stimulated glucose uptake across a range of insulin concentrations.

EXPERIMENTAL PROCEDURES

Materials—LCACoA standards (C16:1, C16:0, C17:0, C18:2, C18:1, and C18:0), diacylglyceride standards, and ceramide standards (C6:0,

[1] The abbreviations used are: IRS-1, insulin receptor substrate-1; IR, insulin receptor; PI3-kinase, phosphatidylinositol 3-kinase; PKC, protein kinase C; DAG, diacylglycerol; LCACoA, long-chain acyl-CoA; LC/MS/MS, liquid chromatography tandem mass spectrometry; MOPS, 4-morpholinepropanesulfonic acid; TNFα, tumor necrosis factor α.

C16:0, C18:0) were purchased from Sigma. *N*-Arachidoyl-D-sphingosine and *N*-lignoceroyl-D-sphingosine were purchased from Avanti Polar Lipids (Arlington, AL). Antibody against IRS-1 was purchased from Upstate Biotechnology (Lake Placid, NY). Antibody against the insulin receptor subunit and Zymed phosphotyrosine and rabbit anti-peptide against nPKC-θ were from Santa Cruz Biotechnology (Santa Cruz, CA). Goat anti-mouse IgG antibodies conjugated to horseradish peroxidase were obtained from Caltag Laboratories (Burlingame, CA). Mouse monoclonal antibody against PKC-θ was from Transduction Laboratories (Lexington, KY).

Animals—Male Wistar rats (Charles River, Wilmington, MA) weighing between 250 and 300 g (for the time course study) and 50 and 75 g (for insulin dose response) were housed in an environmentally controlled room with a 12-h light/dark cycle and fed with regular rat chow diet. The rats were catheterized in the right jugular vein and carotid artery; the catheters were externalized through an incision in the skin flap behind their head. The rats were allowed to recover from surgery until they reached preoperative weight (~5–7 days) and were fasted overnight (~15 h) before the infusion experiment. All procedures were approved by the Yale University Animal Care and Use Committee.

Intralipid Time Course Studies—The rats were divided randomly into five study groups (6–8 rats/group). The control group was infused with isotonic saline solution for 5 h. The other groups were infused with a 20% triglycerides emulsion (Liposyn II, Abbott Laboratories, North Chicago, IL) (5 ml/kg/h) combined with heparin (6 units/h) for 1, 3 and 5 h. A fifth wash-out group was infused with lipid/heparin for 5 h, which was then discontinued and followed with an isotonic saline infusion for another 3 h. Identical studies were performed for muscle DAG analysis (3–9 rats/group) with the addition of a 4-h lipid/heparin infusion group ($n = 4$). At the end of the infusions, rats were anesthetized with pentobarbital (50 mg/kg); soleus muscle samples, rapidly dissected and freeze-clamped *in situ*, were stored at −70 °C for measurement of fat metabolites. Soleus muscle was selected for all studies because it consists of mostly type 1 fiber, which is highly insulin-responsive and best reflects insulin action in human skeletal muscle (10, 11). To study the effect of fatty acids on insulin signaling in muscle at the same time points, we performed another set of identical parallel studies in five groups (basal, 1, 3, an 5 h lipid/heparin infusion and 3 h wash-out) under conditions identical to those described above, adding a 20-min hyperinsulinemic euglycemic clamp following the lipid/heparin or saline infusion. In these studies an intravenous bolus (150 milliunits/kg for 45 s, 75 milliunits/kg for another 45 s) of insulin (humulin regular insulin, Eli Lily, Indianapolis, IN) was followed by a constant insulin infusion at 10 milliunits/kg/min, with plasma glucose concentration clamped at 5.5 mM using a variable infusion of glucose (50g/dl) to maintain euglycemia as described previously (11). At the end of the clamps, rats were anesthetized with pentobarbital (50 mg/kg). Soleus muscle samples were rapidly dissected, freeze-clamped *in situ*, and stored at −70 °C for insulin signaling assays. Rats were euthanized with a lethal dose of pentobarbital.

Extraction of LCACoAs, DAGs, and Ceramides from Tissue Samples—LCACoAs were extracted from frozen tissue samples (~100 mg) and purified using a solid phase extraction method described previously by Deutsch *et al.* (15) with minor modifications for desalting. A known amount of heptadecanoyl-CoA was added as an internal standard. OPC columns (Applied Biosystems, Foster City, CA) were used for solid phase extraction. Samples were dissolved in 100 μl of methanol/H$_2$O for LC/MS/MS analysis.

DAGs and ceramides were extracted from frozen tissue (~100 mg) with chloroform/methanol (2:1, v/v) containing 0.01% butylated hydroxytoluene. Prior to the extraction, known amounts of 1,3-dipentadecanoin, triheptadecanoin, and hexanoylsphingosine were added as internal standards. Extracted samples were evaporated to dryness and redissolved in 1 ml of hexane-methylene chloride-ethyl ether (95:5:0.5, v/v/v). DAGs were isolated from triglycerides by use of a diol bonded-phase SPE column (Waters, Inc., Milford, MA) under vacuum, as described previously (16). Briefly, the SPE column was preconditioned with 4 ml of hexane. The lipid extract was then placed on the column, and triglycerides were eluted with 8 ml of hexane-methylene chloride-ethyl ether (89:10:1, v/v/v). DAGs were eluted with 8 ml of hexane-ethyl acetate (85:15, v/v) into a second set of collection tubes. The solvent was evaporated to dryness under vacuum and redissolved in 0.5 ml of hexane-ethyl acetate (85:15, v/v) for LC/MS/MS analysis. Monitoring for the presence of triheptadecanoin in the DAG fraction assessed the separation of triglycerides from DAGs.

LC/MS/MS Analysis of LCACoAs, DAGs, and Ceramides—A benchtop tandem mass spectrometer, API 3000 (PerkinElmer Life Sciences), interfaced with a TurboIonspray ionization source or atmospheric pres-
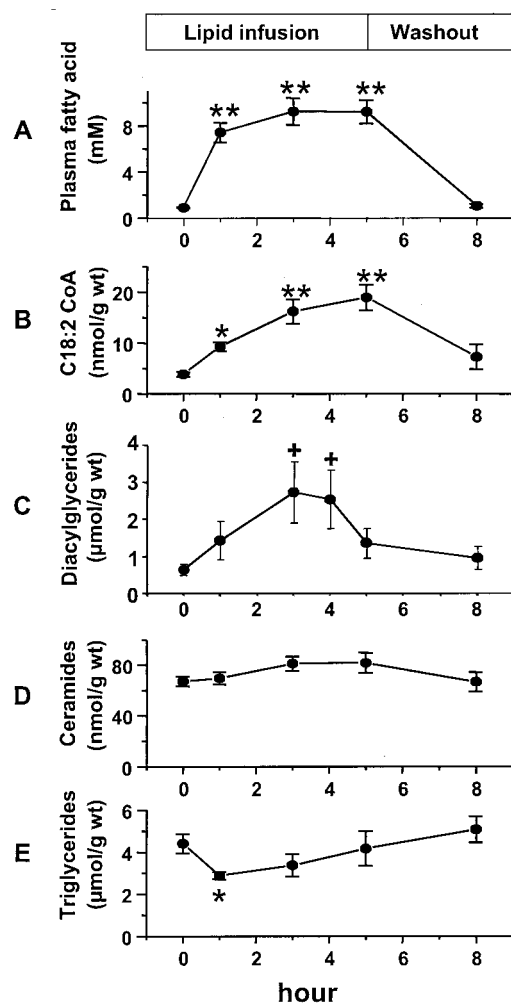

FIG. 1. **Time course for plasma fatty acid and intracellular fat metabolite concentrations in soleus muscles during lipid infusion.** *A*, plasma fatty acid concentrations; *B*, LCACoA concentrations; *C*, diacylglyceride concentrations; *D*, ceramide concentrations; *E*, triglyceride concentrations. Values are means ± S.E. for 6–10 experiments. *, $p < 0.05$ *versus* control groups; +, $p \leq 0.006$, and **, $p < 0.001$ *versus* base line.

sure chemical ionization source was used. Peripherals included a PerkinElmer series 200 micro-pump and an autosampler. LCACoAs were ionized in negative electrospray mode. Doubly charged ions and corresponding product ions were chosen as transition pairs for each CoA species (C16:1, C16:0, C18:2, C18:1, and C18:0) for selective reactions monitoring (SRM) quantitation. Total LCACoAs contents were obtained from the sum of individual species. Methanol/H$_2$O (60/40) was used as continuous flow at 300 μl/min, and 5 μl of sample was injected for analysis. DAGs (derived from C16:1, C16:0, C18:2, C18:1, and C18:0) and ceramides (C16:0, C18:0, C20:0, C22:0, C24:1, C24:0) were ionized in positive atmospheric pressure chemical ionization mode. [M+H-18]$^+$/ product ions from corresponding fatty acid moiety were monitored for SRM quantitation for DAGs. [M+H-18]$^+$/264.3 were monitored for ceramide species for quantitation. The same mobile phase was used for LCACoAs at 300 μl/min and 5 μl of sample injected.

In Vitro Muscle Studies—After a 5-h infusion with glycerol (as control) or lipid/heparin at 85 μl/kg/min, rats were anesthetized with an intravenous injection of sodium pentobarbital (50 mg/kg). Soleus muscles were isolated from the rats and preincubated in oxygenated (95% O$_2$, 5% CO$_2$) Krebs-Henseleit bicarbonated (KHB) buffer containing 2 mM pyruvate, 36 mM mannitol, and 0.1% bovine serum albumin (preincubation buffer) to recover for 30 min at 18 °C. The soleus muscles were then incubated at 29 °C in oxygenated preincubation buffer with various concentration of insulin (0, 50, 1,000, or 10,000 microunits/ml) for 35 min. After incubation, the muscles were rinsed with ice-cold saline and freeze-clamped in liquid nitrogen for analysis of insulin-stimulated IRS-1 tyrosine phosphorylation and insulin-stimulated IRS-1-associated PI3-kinase activity. To measure the insulin-stimulated

A LCACoAs profile

B DAG profile

FIG. 2. **Time course for the concentration profiles of LCACoAs and DAG in soleus muscles during the lipid infusion.** *A*, individual LCACoAs species were quantitated: *C16:1*, palmitoleoyl-CoA; *C16:0*, palmitoyl-CoA; *C18:2*, linoleoyl-CoA; *C18:1*, oleoyl-CoA; and *C18:0*, stearoyl-CoA. Values are means ± S.E. for 6–10 experiments. *, $p < 0.05$ *versus* control group; **, $p < 0.001$ *versus* control group. *B*, DAG species were abbreviated as two contributing fatty acyl groups. *S*, stearoyl; *O*, oleoyl; *L*, linoleoyl; *P*, palmitoyl; *Po*, palmitoleoyl. Values are means ± S.E. for 3–9 experiments. *, $p < 0.05$ *versus* control group.
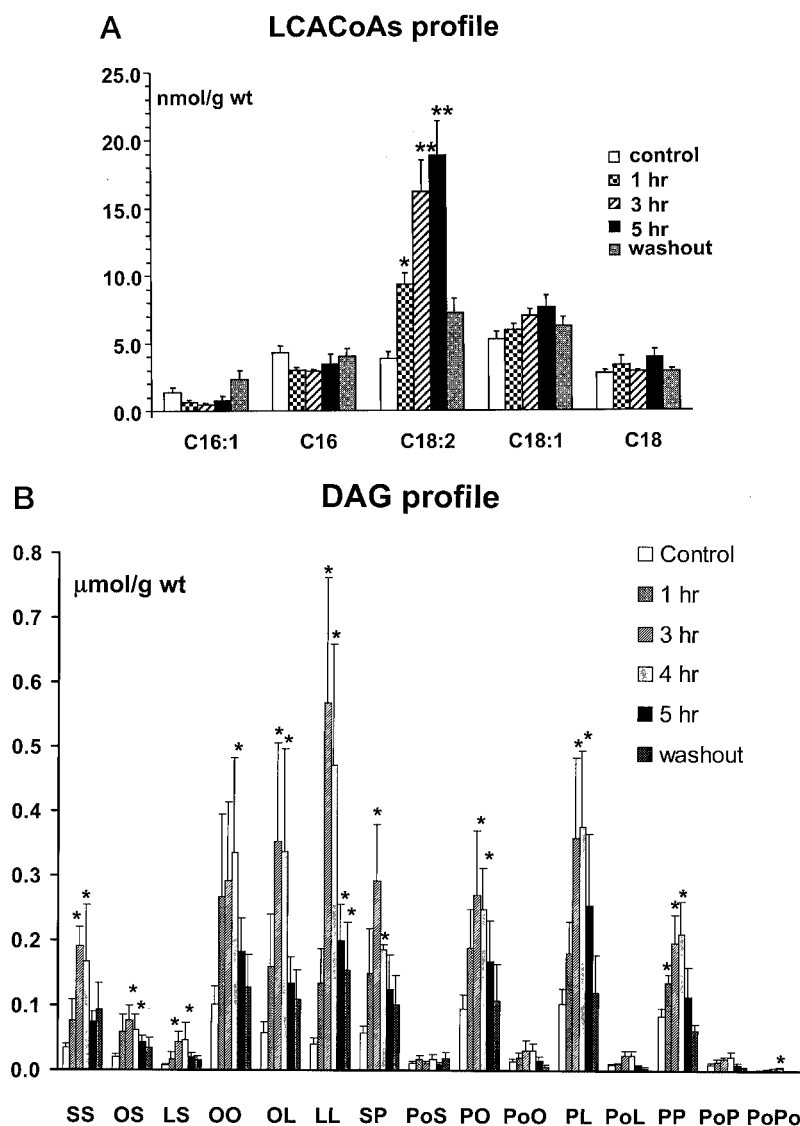
glucose uptake in the muscle, soleus muscles were preincubated at 29 °C with various concentrations of insulin (0, 50, 1,000, or 10,000 microunits/ml) for 35 min followed by incubation in KHB buffer containing 1 mM [^{3}H]2-deoxyglucose and 39 mM [1-^{14}C]mannitol for an additional 20 min. For IRS-1 serine phosphorylation analysis, after a 5-h lipid infusion, soleus muscles were freeze-clamped *in situ* and kept in liquid nitrogen until analysis.

Insulin Signaling Assays—Muscle samples were ground under liquid nitrogen and homogenized in a ice-cold Hepes buffer, pH 7.4, containing 150 mM NaCl 50 mM β-glycerol phosphate, 2 mM dithiothreitol, 1 mM NaVO$_4$, 2 mM EDTA, 1 mM phenylmethylsulfonyl fluoride, 1% Triton-100, 10% glycerol, and 10 μg/ml aprotinin. The homogenates were centrifuged at 20,500 × g for 1 h. Supernatants were collected, and protein concentration was measured with the Bradford protein assay reagent (Bio-Rad). Muscle homogenates (4 mg protein) were immunoprecipitated with 4 μg of anti-IRS-1 antibody for 18 h for IRS-1 tyrosine phosphorylation and PI3-kinase activity assay or with 4 μg of anti-IR antibody for IR tyrosine phosphorylation.

IR and IRS-1 Tyrosine Phosphorylation Assays—Immunoprecipitates were washed three times by brief centrifugation and gentle resuspension in ice-cold homogenization buffer plus 0.1% SDS. Immunoprecipitates were subjected to SDS-PAGE on a 4–12% gradient gel. Proteins were transferred to nitrocellulose membrane using a semidry electro-blotter (Owl Separation System, Portsmouth, NH). The membranes were immunoblotted with anti-phosphotyrosine antibody, and bands were visualized using enhanced chemiluminescence (Amersham Biosciences) and quantified by densitometry (Amersham Biosciences). The membrane was stripped with 100 mM glycine, pH 3.0, and reblotted with anti-IRS-1 antibody to determine the amount of IRS-1 proteins.

IRS-1 serine phosphorylation was measured using a site-specific antibody, phospho-Ser^{307}, generated in Dr. Morris White's laboratory (17). Immunoprecipitation and Western blotting procedures were the same as for IRS-1 tyrosine phosphorylation.

PI3-kinase Activity Assay—The immunoprecipitates were washed twice with phosphate-buffered saline, twice with 100 mM Tris, pH 7.5, containing 500 mM LiCl$_2$, and twice with 10 mM Tris containing 150 mM NaCl and 1 mM EDTA. 100 μM Na$_3$VO$_4$ was included in all the wash buffers. Kinase reactions were done as described previously (11). ^{32}P was captured with a storage phosphor-screen, and the screen was scanned with a Storm system. Images were analyzed and quantified using ImageQuant software.

PKC-θ Translocation Assay—100 mg of soleus muscle was homogenized and extracted in 4× (w/v) ice cold 20 mM MOPS, pH 7.5, 250 mM mannitol, 1.2 mM EGTA, 1 mM dithiothreitol, 2 mM phenylmethylsulfonyl fluoride, leupeptin (200 μg/ml), and 2 mM benzamidine. The homogenate was solubilized by hand for 2 min and centrifuged at 4 °C for 10 min at 100,000 × g. Separation of cytosol and membrane fraction was done as described previously (18). 5 (cytosolic) or 10 μg (particulate) of protein was loaded and subjected to SDS-PAGE (10% gel, 187 V). Proteins separated on the gels were electrophoretically transferred to polyvinylidene difluoride filter membranes (Amersham Biosciences) in 19 mM Tris, pH 8.9, buffer containing 140 mM glycine at 90 V for 90 min. Polyvinylidene difluoride membranes were probed with 0.625 μg/ml anti-PKC-θ antibody (Transduction Laboratories) for 2 h at room temperature, followed by horseradish peroxidase-conjugated goat anti-mouse antibody (1:5,000) for 2 h. PKC isozymes visualized by enhanced chemiluminescence reagents and quantitated by densitometry using a Medical Dynamics Personal Densitometer SI and IP Lab Gel H software (Signal Analytics, Vienna, VA). Individual band densities were adjusted for inter-gel variability using the standard, and the amount of PKCθ in

each fraction were calculated according to the total amount of protein in the final volume of supernatant extracted.

Analytical Procedures—Plasma fatty acid concentration was determined with an acyl-CoA oxidase-based colorimetric kit (Wako NEFA-C, Wako Pure Chemicals, Osaka, Japan). Tissue triglycerides were extracted by adapting the method described by Storlien *et al.* (19), and triglyceride content was measured using a kit from Sigma.

Statistical Analysis—Data were expressed as means ± S.E. Analysis of data using analysis-of-variance with one-way post-hoc tests (Fisher's protected least significant difference) was done to determine the differences between control and different time courses of lipid infusion groups at a minimum $p < 0.05$ threshold.

RESULTS

Basal plasma fatty concentration increased rapidly following the lipid/heparin infusion and remained constant until the saline wash-out period during which time it returned to baseline concentration (Fig. 1*A*). This increase in plasma fatty acid concentration in the lipid-infused group resulted in increases in both intramuscular LCACoAs and DAG concentration in the soleus muscle compared with the control group (Fig. 1, *B* and *C*). Although the LCACoA continued to increase throughout the lipid infusion, the DAGs reached a peak concentration at 3–4 h and then surprisingly decreased to basal concentrations despite continued lipid infusion (Fig. 1*C*). In contrast, lipid infusion had no effect on intramyocellullar ceramide content (Fig. 1*D*) or muscle triglyceride (Fig. 1*E*) content except at the 1-h time point, at which time the concentration decreased compared with base line. The increase in total LCACoA concentration could be accounted for entirely by a selective increase in C18:2 CoA (major fatty acid composition in liposyn II) (3.86 ± 0.46 nmol/g of weight for control group, 9.30* ± 0.87, 16.17** ± 2.37, and 18.89** ± 2.51 nmol/g of weight after a 1-h, 3-h, and 5-h lipid infusion and 7.22 ± 1.22 nmol/g of weight after wash-out period; *, $p < 0.05$ *versus* control; **, $p < 0.001$ *versus* control; Fig. 2*A*). In contrast the transient ~3–4-fold increase in total DAG content at 3–4 h (0.65 ± 0.14 μmol/g of weight for control group, 1.43 ± 0.51, 2.73 ± 0.83[+], 2.54 ± 0.79[+], 1.36 ± 0.40, 0.96 ± 0.31 μmol/g of weight for 1-h, 3-h, 4-h, 5-h and wash-out groups, respectively; +, $p \leq 0.006$ *versus* control) could be attributed to an increase in virtually all DAG species (Fig. 2*B*). These increases in intracellular LCACoA and DAG concentrations were associated with PKC-θ activation, as reflected by a significant reduction in the fraction of PKC-θ in the cytosol and a significant increase in the PKC-θ membrane-associated/cytosol fraction after 5 h of lipid infusion (both $p = 0.04$ *versus* control group; Fig. 3). There was also a reduction in total PKC-θ content, which is consistent with previous observations in a high-fat fed rat model that had increased intramuscular lipid accumulation (20).

The increase in intracellular fatty acyl-CoA and PKC-θ activation were also associated with a significant impairment in insulin-stimulated IRS-1 tyrosine phosphorylation and IRS-1-associated PI3-kinase activity after 5 h of lipid infusion (Fig. 4). These changes were associated with a 1.6-fold increase ($p = 0.002$ *versus* control) in IRS-1 Ser[307] phosphorylation following 5 h of lipid infusion (Fig. 5). In contrast lipid infusion did not inhibit insulin-stimulated insulin receptor tyrosine phosphorylation (Fig. 4).

Following the 3-h lipid wash-out period, intracellular 18:2 acyl-CoA returned to base-line concentrations, and PKC-θ activity returned to normal (Figs. 1 and 3). In parallel with these results insulin-stimulated IRS-1 tyrosine phosphorylation and IRS-1-associated PI3-kinase activity also returned to normal.

To determine whether higher concentrations of insulin could overcome these lipid-induced defects in insulin signaling and action, we also examined insulin-stimulated muscle glucose uptake and insulin signaling across a wide range of insulin concentrations (50, 1,000, and 10,000 microunits/ml) in an *in*
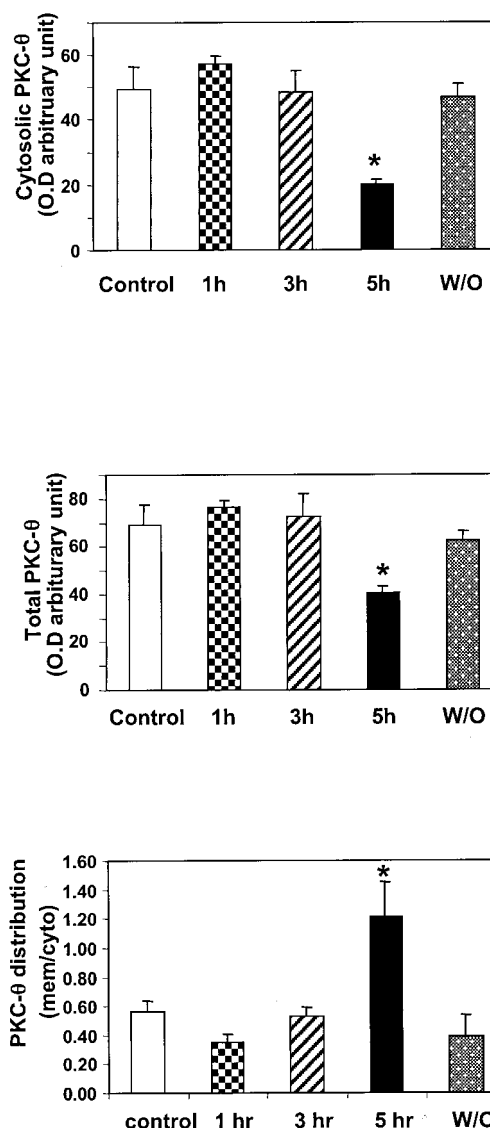
FIG. 3. **Time course for the effects of fatty acids on PKC-θ activity in soleus muscle *in vivo*.** PKC-θ protein levels were determined in the cytosolic and membrane fraction by immunoblotting with PKC-θ specific antibodies. Total PKC-θ levels were calculated from the sum of cytosolic and membrane-associated amounts, and PKC-θ distribution was expressed as the ratio of membrane-associated to cytosolic amounts. *W/O*, without. Values are means ± S.E. for 6–10 experiments. *, $p < 0.05$ *versus* control groups.

vitro soleus muscle preparation following 5 h of either lipid or glycerol infusion. Consistent with our previous results, 5 h of lipid infusion induced a profound defect in insulin-stimulated glucose uptake, which occurred across all insulin concentrations (Fig. 6). This reduction in insulin-stimulated glucose uptake was paralleled by similar reductions in insulin-stimulated IRS-1 tyrosine phosphorylation and IRS-1-associated PI3-kinase activity across all insulin concentrations, but there was no change in insulin receptor tyrosine phosphorylation (Fig. 7). Taken together these results demonstrates that fatty acids induce a defect in insulin activation of PI3-kinase at the level of IRS-1 tyrosine phosphorylation that cannot be overcome with supraphysiologic concentrations of insulin.

DISCUSSION

To examine the possible roles of fatty acyl-CoA, diacylglycerol, ceramides, and triglycerides in mediating fatty acid induced insulin resistance in skeletal muscle, we assessed the intracellular concentration of these metabolites at different
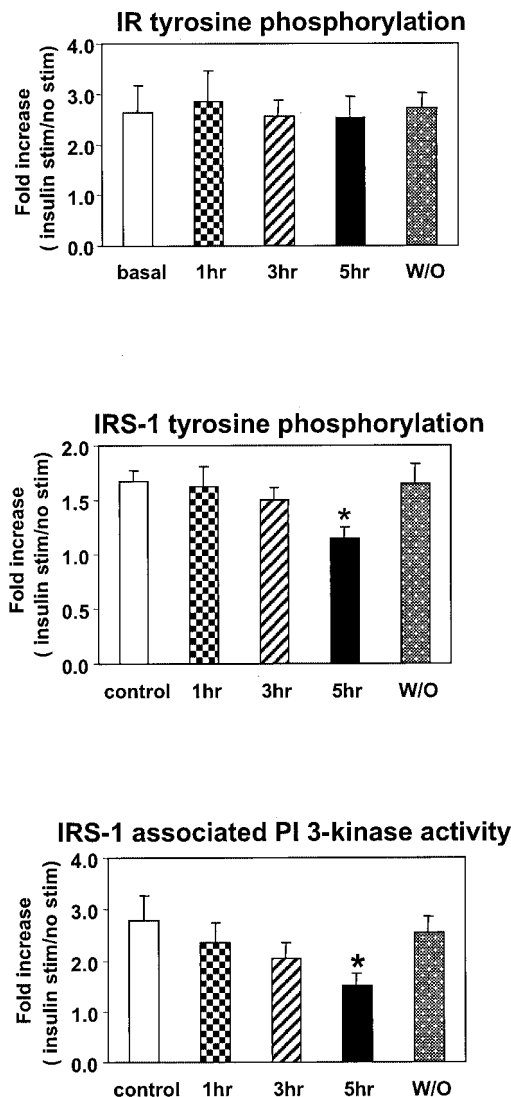
Mechanism of Fatty Acid-induced Insulin Resistance

IR tyrosine phosphorylation

IRS-1 tyrosine phosphorylation

IRS-1 associated PI 3-kinase activity

FIG. 4. **Time course for the effects of fatty acids on insulin signaling in soleus muscle *in vivo*.** Insulin-stimulated IR tyrosine phosphorylation, insulin-stimulated IRS-1 tyrosine phosphorylation, and insulin-stimulated IRS-1-associated PI3-kinase activity are all expressed as fold increase of insulin stimulation over basal states. Values are means ± S.E. for 5–8 experiments. *, $p < 0.05$ *versus* control groups.

FIG. 5. **Effects of fatty acids on IRS-1 Ser[307] phosphorylation in soleus muscle *in vivo*.** *A*, IRS-1 Ser[307] phosphorylation was detected with a polyclonal antibody raised specifically for phosphorylated Ser[307] (*upper panel*). Nitrocellulose membranes were stripped and reprobed with IRS-1 antibody to ensure equal amount of protein loading (*lower panel*). *IP*, immunoprecipitate; *INS*, insulin; *Gly*, glycerol; *WB*, Western blot. *B*, degree of IRS-1 Ser[307] phosphorylation in glycerol- and lipid-infused groups. Values are means ± S.E. from six rats for each group. *, $p < 0.05$ *versus* glycerol-infused rats.

FIG. 6. **Insulin dose response for the effects of fatty acids on insulin-stimulated 2-deoxyglucose uptake in soleus muscle *in vitro*.** Soleus muscles were isolated from glycerol- or lipid-infused rats. They were then incubated with insulin at 0, 50, 1000, and 10,000 microunits/ml. The rate of 2-deoxyglucose uptake was measured and expressed as fold change over non-insulin-stimulated groups. Values are means ± S.E. from 6–9 experiments. *, $p < 0.05$ *versus* glycerol-infused rats.

time intervals during a lipid infusion in awake rats. The changes in these fatty acid metabolite concentrations were then compared with changes in insulin-stimulated insulin receptor tyrosine phosphorylation, IRS-1 tyrosine phosphorylation, IRS-1-associated PI3-kinase activity, and PKC-θ translocation. We found that during the lipid infusion intra- myocellular C18:2 CoA concentration increased by ~6-fold and that it was the only intracellular fatty acyl-CoA to increase. Because the infused intralipid consisted mostly of C18:2 fatty acids, these data strongly suggest that this intracellular fatty acyl-CoA was derived from the infused lipid. Following the increase in intracellular C18:2 CoA, there was a ~3-fold increase in intracellular DAG, which peaked at 3–4 h and then surprisingly declined despite persistent elevation in plasma fatty acid concentrations. In contrast to the fatty acyl-CoA, which consisted mostly of C18:2 fatty acids, the increase in DAG consisted of virtually all measured fatty acids. Taken together these data suggest that an increase in intracellular fatty acyl-CoA activates a phospholipase that leads to production of DAG from endogenous lipid sources, which might ex-
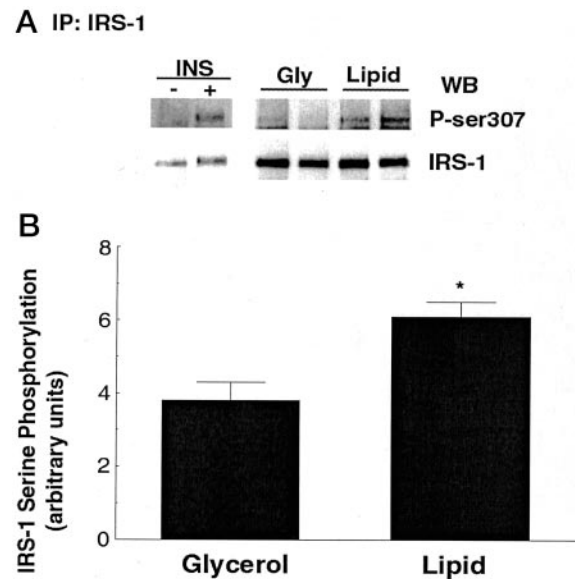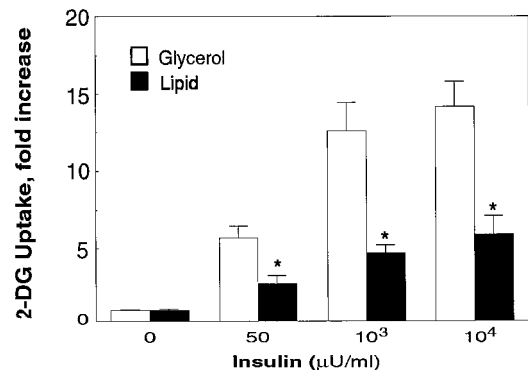
plain the observed decrease in intramuscular triglyceride content during the first couple of hours of the lipid infusion. In contrast to the increases in intracellular fatty acyl-CoA and DAG, there were no significant increases in intracellular ceramides or triglyceride concentrations during the 5-h lipid infusion, which suggests that these metabolites do not play a major role in mediating fatty acid-induced insulin resistance in skeletal muscle.

In parallel with the increases in intracellular fatty acyl-CoA, we observed a ~30% reduction in insulin activation of IRS-1 tyrosine phosphorylation and an ~50% reduction in IRS-1-associated PI3-kinase activity after 5 h of lipid infusion, which coincided with activation of PKC-θ. These data might explain the 3–5 h delay for fatty acid-induced insulin resistance in skeletal muscle resulting from an intralipid/heparin infusion
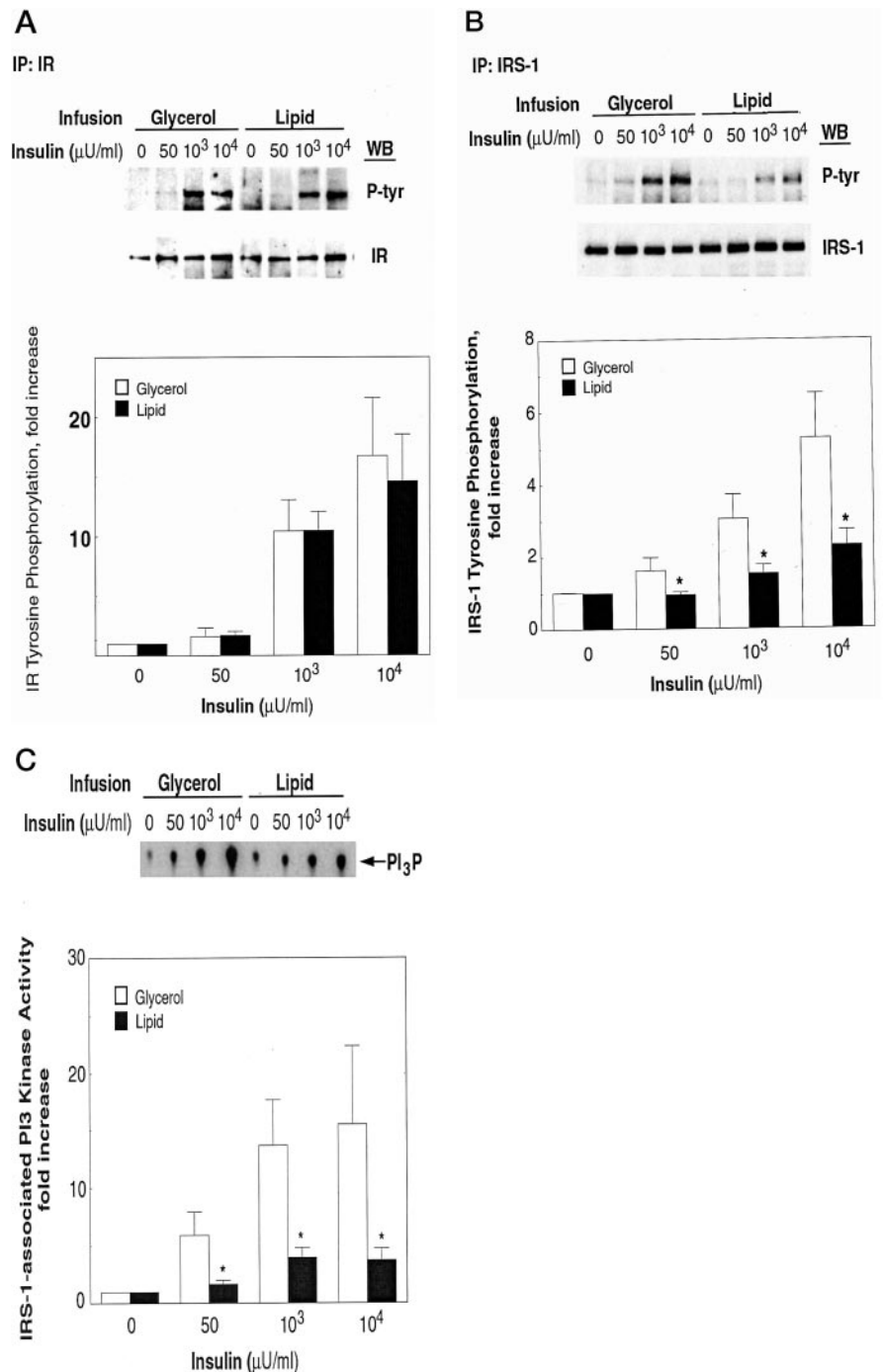
FIG. 7. **Insulin dose response for the effects of fatty acids on insulin signaling in soleus muscle *in vitro*.** *A*, IR tyrosine phosphorylation was detected with phosphotyrosine-specific antibody (*upper panel*). Nitrocellulose membranes were stripped and reprobed with insulin receptor antibody to ensure equal amount of protein loading (*lower panel*). The *bar graph* shows the degree of IR tyrosine phosphorylation in glycerol- or lipid-infused soleus muscle *in vitro*. *IP*, immunoprecipitate. *B*, IRS-1 tyrosine phosphorylation was detected with phosphotyrosine-specific antibody (*P-tyr*, *upper panel*). Nitrocellulose membranes were stripped and reprobed with IRS-1 antibody to ensure equal amounts of protein loading (*lower panel*). The *bar graph* shows the degree of IRS-1 tyrosine phosphorylation in glycerol- or liposyn-infused soleus muscle *in vitro*. *WB*, Western blot. *C*, IRS-1-associated PI3-kinase activity was detected by measuring ^{32}P incorporation into phosphatidylinositol (*PI$_3$P*). The *bar graph* shows the IRS-1-associated PI3-kinase activity in glycerol- or liposyn-infused soleus muscle *in vitro*. Values are means ± S.E. from eight independent experiments. *, $p < 0.05$ *versus* glycerol-infused rats.

(8, 9). In contrast, the lipid infusion had no effect on insulin receptor tyrosine phosphorylation. Overall these data demonstrate that increases in plasma fatty acid concentration inhibit insulin activation of IRS-1-associated PI3-kinase at the level of IRS-1, possibly though activation of PKC-θ, a known serine kinase. To gain further insights into this mechanism we assessed IRS-1 Ser[307] phosphorylation. Previous *in vitro* studies by Aguirre *et al.* (17) demonstrated that IRS-1 Ser[307] phosphorylation is a critical site in mediating TNFα-induced insulin resistance in Chinese hamster ovary cells. When IRS-1 Ser[307] was mutated to IRS-1 Ala[307], these cells were protected from TNFα-induced insulin resistance. Indeed, in the present study we found that after 5 h of lipid infusion there was a 1.6-fold increase in IRS-1 Ser[307] phosphorylation in soleus muscle, which suggests that fatty acids may mediate insulin resistance through the same common final pathway as TNFα (21).

To determine whether higher concentrations of insulin could overcome these fatty acid-induced defects in insulin signaling and action, we also examined these parameters *in vitro*, across a wide range of insulin concentrations, in soleus muscles obtained from rats following 5 h of either lipid or glycerol infusion. Consistent with our current and previous *in vivo* results, 5 h of lipid infusion induced a profound defect in insulin-stimulated glucose uptake (9–11), which occurred across all insulin concentrations. This reduction in insulin-stimulated glucose uptake was paralleled by similar reductions in insulin-stimulated IRS-1 tyrosine phosphorylation and IRS-1-associated PI3-kinase activity across all insulin concentrations, but there was no change in insulin-stimulated IR tyrosine phosphorylation. Taken together these results demonstrate that the fatty acid-induced inhibition of insulin-stimulated glucose transport activity in muscle can be explained for the most part

by decreased activation of PI3-kinase at the level of IRS-1 tyrosine phosphorylation, which cannot be overcome with supraphysiologic concentrations of insulin.

In conclusion, these data provide new insights into the pathogenesis of fat-induced insulin resistance in skeletal muscle and support the hypothesis that an increase in plasma fatty acid concentration results in an increase in intracellular fatty acyl-CoA and DAG concentrations, which then results in activation of PKC-θ leading to increased IRS-1 Ser[307] phosphorylation. These changes in turn result in decreased IRS-1 tyrosine phosphorylation and decreased activation of IRS-1-associated PI3-kinase, resulting in decreased insulin-stimulated glucose transport activity.

REFERENCES

1. Kraegen, E. W., Cooney, G. J., Ye, J. M., Thompson, A. L., and Furler, S. M. (2001) *Exp. Clin. Endocrinol. Diabetes* **109,** Suppl 2, S189–S201
2. Kim, J. K., Gavrilova, O., Chen, Y., Reitman, M. L., and Shulman, G. I. (2000) *J. Biol. Chem.* **275,** 8456–8460
3. Kim, J. K., Fillmore, J. J., Chen, Y., Yu, C., Moore, I. K., Pypaert, M., Lutz, E. P., Kako, Y., Velez-Carrasco, W., Goldberg, I. J., Breslow, J. L., and Shulman, G. I. (2001) *Proc. Natl. Acad. Sci. U. S. A.* **98,** 7522–7527
4. Pan, D., Lillioja, S., Kriketos, A., Milner, M., Baur, L., Bogardus, C., Jenkins, A., and Storlien, L. (1997) *Diabetes* **46,** 983–988
5. Krssak, M., Falk Petersen, K., Dresner, A., DiPietro, L., Vogel, S. M., Rothman, D. L., Roden, M., and Shulman, G. I. (1999) *Diabetologia* **42,** 113–116
6. Perseghin, G., Scifo, P., De Cobelli, F., Pagliato, E., Battezzati, A., Arcelloni, C., Vanzulli, A., Testolin, G., Pozza, G., Del Maschio, A., and Luzi, L. (1999) *Diabetes* **48,** 1600–1606
7. Jacob, S., Machann, J., Rett, K., Bretchel, K., Volk, A., Renn, W., Maerker, E., Matthaei, S., Schick, F., Claussen, C. D., and Harring, H. U. (1999) *Diabetes* **48,** 1113–1119
8. Boden, G., and Chen, X. (1995) *J. Clin. Invest.* **96,** 1261–1268
9. Roden, M., Price, T. B., Perseghin, G., Petersen, K. F., Rothman, D. L., Cline, G. W., and Shulman, G. I. (1996) *J. Clin. Invest.* **97,** 2859–2865
10. Dresner, A., Laurent, D., Marcucci, M., Griffin, M. E., Dufour, S., Cline, G., Slezak, L. A., Andersen, D. K., Hundal, R. S., Rothman, D. L., Petersen, K. F., and Shulman, G. I. (1999) *J. Clin. Invest.* **103,** 253–259
11. Griffin, M. E., Marcucci, M. J., Cline, G. W., Bell, K., Barucci, N., Lee, D., Goodyear, L. J., Kraegen, E. W., White, M. F., and Shulman, G. I. (1999) *Diabetes* **48,** 1270–1274
12. Randle, P. J., Garland, P. B., Hales, C. N., and Newsholme, E. A. (1963) *Lancet* **i,** 785–789
13. Randle, P. J., Newsholme, E. A., and Garland, P. B. (1964) *Biochem. J.* **93,** 652–665
14. Roden, M., Krssak, M., Stingl, H., Gruber, S., Hofer, A., Furnsinn, C., Moser, E., and Waldhausl, W. (1999) *Diabetes* **48,** 358–364
15. Deutsch, J., Grange, E., Rapoport, S. I., and Purdon, A. D. (1994) *Anal. Biochem.* **220,** 321–323
16. Pacheco, Y. M., Perez-Camino M. C., Cert A., Montero E., and Ruiz-Gutierrez, V. (1998) *J. Chromatogr. B Biomed. Sci. Appl.* **714,** 127–132
17. Aguirre, V., Uchida, T., Yenush, L., Davis, R., and White, M. (2000) *J. Biol. Chem.* **275,** 9047–9054
18. Laybutt, D. R., Schmitz-Peiffer, C., Saha, A. K., Ruderman, N. B., Biden, T. J., and Kraegen, E. W. (1999) *Am. J. Physiol.* **277,** E1070–E1076
19. Storlien, L. H., Jenkins, A. B., Chisholm, D. J., Pascoe, W. S., Khouri, S., and Kraegen, E. W. (1991) *Diabetes* **40,** 280–289
20. Schmitz-Peiffer, C., Browne, C. L., Oakes, N. D., Watkinson, A., Chisholm, D. J., Kraegen, E. W., and Biden, T. J., (1997) *Diabetes* **46,** 169–178
21. Hotamisligil, G. S., Peraldi, P., Budavari, A., Ellis, R., White, M. F., and Spiegelman, B. M. (1996) *Science* **271,** 665–668

Mechanism by Which Fatty Acids Inhibit Insulin Activation of Insulin Receptor Substrate-1 (IRS-1)-associated Phosphatidylinositol 3-Kinase Activity in Muscle

Chunli Yu, Yan Chen, Gary W. Cline, Dongyan Zhang, Haihong Zong, Yanlin Wang, Raynald Bergeron, Jason K. Kim, Samuel W. Cushman, Gregory J. Cooney, Bronwyn Atcheson, Morris F. White, Edward W. Kraegen and Gerald I. Shulman

Access the most updated version of this article at doi: 10.1074/jbc.M200958200

Alerts:
- When this article is cited
- When a correction for this article is posted

Click here to choose from all of JBC's e-mail alerts

This article cites 21 references, 12 of which can be accessed free at
http://www.jbc.org/content/277/52/50230.full.html#ref-list-1